TIJMET 002 (2019) 08-15

The International Journal of

Materials and Engineering Technology

ISSN: 2667-4033
TIJMET ID: 190201002 (8 pages)
Type of the Paper: Article
Received 16.01.2019 Revised: 06.02.2019 Accepted: 08.02.2019 Published (Online): 13.02.2019
Journal homepage: http://dergipark.gov.tr/tijmet

PRESSURE DISTRIBUTION OF FLUID IN A JOURNAL BEARING CONSIDERING THE EFFECT OF SIDE OR END LEAKAGE, USING THE TWO DIMENSIONAL REYNOLDS MODEL

I. D. ERHUNMWUN[1] and J. A. AKPOBI[2]

[1,2]Department of Production Engineering, University of Benin, P.M.B. 1154, Benin City, Nigeria.
Email: [1]iredia.erhunmwun@uniben.edu, [2]john.akpobi@uniben.edu

Abstract

This paper presents numerical solution to the pressure distribution of a fluid in a hydro-dynamically lubricated journal bearing using the classical Reynolds equation that models the effect of side or end leakage i.e., there is flow in the z-direction in bearings. The finite element method was used to analyze the flow. Two dimensional interpolation functions were used in the modelling and discretization of the domain of analysis. The result obtained from this research shows that the pressure increases from the ambient pressure which is taken to be zero at an angular displacement of 0^o and increases significantly till 135^o. At this point, the pressure becomes maximum. Thereafter, it begins to drop until it gets to 180^o where the pressure becomes the same as the ambient pressure. From this point onward, we begin to experience negative pressure. The negative pressures in this regard are those that are below the ambient pressure.

Keywords: Finite Element Method, Journal Bearing, Reynolds Equation, End Leakage

1. Introduction

The classical Reynolds equation for one dimensional flow has been solved by many authors using different mathematical tools. In all, the problem have been solved with the assumption that there is no flow in the z-direction i.e., there is no side leakage. This assumption is theoretically feasible but in practice, there must be flow of the lubricant along the z-direction. There is no general analytic solution to the classical Reynolds equation that models the effect of side or end leakage [1]; however, approximate solutions have been obtained by using electrical analysis, mathematical summations, relaxation methods and numerical and graphical methods.

A comparative study of pressure distribution and load capacity of a cylindrical bore journal bearing using both analytical method and finite element method has been carried out [2]. An approximate analytical solution to Reynolds equation for isothermal finite length journal bearing by means of the regular perturbation method has been proposed [3]. $(L/D)^2$ was used as the perturbation parameter. Benasciutti *et al.* [4] presented a numerical approach for the analysis of hydrodynamic radial journal bearings. The effect of shaft and housing elastic deformation on pressure distribution within oil film was investigated. Dwivedi *et al.* [5] tried to find out the effect of eccentricity ratio on the pressure distribution pattern by constructing the analytical model of infinite short bearing approximation and solving it with the help of MATLAB. Their results have good agreement against the works of [6] and [7]. An exact analytical solution to the Reynolds equation for the finite journal bearing

lubrication was presented by Sfyris & Chasalevris [8]. In their work, the Reynolds equation for the pressure distribution of lubricant in a journal bearing with finite length was solved analytically using the method of separation of variables in an additive and a multiplicative form. In their study Mane & Soni [9] presented a 3D model of hydrodynamic plain journal bearing using COMSOL Multi-physics 4.3a software. A finite element procedure was developed for the steady-state and dynamic analysis of oil-lubricated cylindrical journal bearing [10]. Again, Priyanka & Veerendra [11] analysed hydrodynamic journal bearings using Computational fluid dynamics (CFD) and fluid structure interaction (FSI) approach in order to find Pressure profile and temperature distribution in the bearing structure, satisfying the boundary conditions. Paras & Ashish [12] presented an experimental study of pressure distribution on hydrodynamic journal bearing with SAE 10W30 multi grade oil using Hydrodynamic Journal Bearing Test Rig (HJBTR). The results were used for experimental calculations and theoretical verification using Raimondi and Boyd charts for practical design. In their study, Gustafson *et al.* [13] derive a novel and rigorous correction to the classical Reynolds lubrication approximation for fluids with viscosity depending upon the pressure. Francisco [14] presents the development of a general discretization scheme for the solution of Reynolds equation with a mass-conserving cavitation model and its application for the numerical simulation of lubricated contacts to be discretized using irregular grids. Fu *et al.* [15] studied how to improve the lubrication in R410A rotary compressor. Verma & Samant [16] carried out an unsteady transient analysis for hydro-dynamically lubricated journal bearing with infinitely long approximation. Results comprising of Minimum lubricant film thickness, Dynamic pressure and load, Wall shear stress, Eccentricity, Temperature distribution and heat flux with respect to time were presented in the analysis graphically with the aid of ORIGION PRO 8.

An investigation on journal bearings subjected to heavy load and slow speed operates in mixed lubrication regime causing contact between the interacting surfaces and resulting in wear was carried out by Muzakkir [17]. The complexity of wear behaviour and lack of unifying theory/model make wear control very challenging. In the work, a methodology was outlined for minimizing wear in journal bearing operating in mixed lubrication regime. Shinde & Nagare [18] carried out an experimental evaluation of performance parameters (such as temperature, frictional torque and coefficient of friction) of journal bearing operating in boundary/ mixed lubrication regimes. Manojkumar *et al.* [19] analysed Elasto-hydrodynamic journal bearing using CFD and fluid structural interactions (FSI) approach. Hamdavi *et al.* [20], carried out theoretical studies and approach for finite fluid film journal bearing. In the research, the oil film pressure, load carrying capacity and attitude angle for plain and grooved short bearing were calculated and compared. Their result shows that applying one groove at inlet bearing surface, there was a decline in the performance of finite fluid film journal bearings.

Sequel to the fact that there is no general analytical solution to the classical Reynolds, this study was presented to prefer a solution to the pressure distribution in a journal bearing considering the effect of side leakage i.e., flows in the z-direction, using the finite element method.

2. Materials and Method

The hydrodynamic theory applied to the hydrodynamic lubricated bearing is mathematically explained by Reynolds's Equation. The classical theory of Reynolds is based on several assumptions that were adopted to simplify the mathematical derivations. Hydrodynamic lubrication can be expressed mathematically in the form of an equation which was originally derived by Reynolds and is commonly known as the 'Reynolds equation'. The classical Reynolds equation for one dimensional flow is given by the eq. 1.

$$\frac{d}{dx}\left(\frac{h^3}{\mu}\frac{dP}{dx}\right) = -6U\frac{dh}{dx} \qquad (1)$$

Eq. 1 neglects side leakage, that is, flow in the z-direction. A similar development is used when side leakage is not neglected. The resulting equation is:

$$\frac{d}{dx}\left(\frac{h^3}{\mu}\frac{dP}{dx}\right) - \frac{d}{dz}\left(\frac{h^3}{\mu}\frac{dP}{dz}\right) = -6U\frac{dh}{dx} \qquad (2)$$

Initial and boundary conditions

The initial and boundary condition for eq. 2,

$$P(\theta, l/2) = P(\theta, -l/2) = P_a \qquad (3)$$

where P_a is the ambient pressure.

For symmetry reasons

$$\left.\frac{\partial P}{\partial \theta}\right|_{0,z} = \left.\frac{\partial P}{\partial \theta}\right|_{2\pi,z} \text{ and } \quad \left.\frac{\partial P}{\partial z}\right|_{\theta,0} = 0 \qquad (4)$$

2.1 Weak formulation for Two Dimensional Journal bearing

In the development of the weak form, we need only consider an arbitrarily typical element. We assume that the domain is such an element which is rectangular and we develop the finite element model of eq. 2 over the domain.

Multiply eq. 2 by the weighted residual and integrate the final equation over the domain which in this case is the area. The result obtained is as shown in eq. 5.

$$-\int_A \frac{\partial w}{\partial x}\frac{\partial P}{\partial x}dA + \int_A \frac{\partial w}{\partial z}\frac{\partial P}{\partial z}dA = -\frac{6\mu U}{h^3}\frac{\partial h}{\partial x} - w\left.\frac{\partial P}{\partial x}\right|_A + w\left.\frac{\partial P}{\partial z}\right|_A \quad (5)$$

Eq. 5 is referred to as the weak form.

2.2 Finite Element Formulation

The weak form in eq. 5 requires that the approximation chosen for P should be at least linear in both x and z so that there are no terms in eq. 5 that are identically zero. Since the primary variable is simply the function itself, the Lagrange family of interpolation functions is admissible. Suppose that P is approximation over a typical finite element domain by the expression

$$\text{Let } P = \sum_{j=1}^{n} P_j \psi_j \text{ and } w = \psi_i \qquad (6)$$

Substitute eq. 6 into eq. 5, we have and factor out $\sum_{j=1}^{n} P_j$, we have,

$$-\sum_{j=1}^{n} P_j \int_A \frac{\partial \psi_i}{\partial x}\frac{\partial \psi_j}{\partial x}dA + \sum_{j=1}^{n} P_j \int_A \frac{\partial \psi_i}{\partial z}\frac{\partial \psi_j}{\partial z}dA = -\frac{6\mu U}{h^3}\frac{\partial h}{\partial x}\int_A \psi_i dA + Q \qquad (7)$$

$$\text{where } Q = -\psi_i \left.\frac{\partial P}{\partial x}\right|_A + \psi_i \left.\frac{\partial P}{\partial z}\right|_A \qquad (8)$$

In matrix form,

$$\left[K^e\right]\left\{P_j\right\} = -\frac{6\mu U}{h^3}\frac{\partial h}{\partial x}\left\{F^e\right\} + \left\{Q^e\right\} \qquad (9)$$

Eq. 9 is referred to as the finite element model of the well-known 2D classical Reynold's equation, where

$$K^e = -\int_A \frac{\partial \psi_i}{\partial x}\frac{\partial \psi_j}{\partial x}dA + \int_A \frac{\partial \psi_i}{\partial z}\frac{\partial \psi_j}{\partial z}dA \quad (10)$$

$$F^e = \int_A \psi_i dA \qquad (11)$$

A linear rectangular element is used in this problem and for the purpose of this research, four elements will be used.

$$\psi_1 = \left(1-\frac{x}{X}\right)\left(1-\frac{z}{Z}\right) \qquad (12)$$

$$\psi_2 = \frac{x}{X}\left(1-\frac{z}{Z}\right) \qquad (13)$$

$$\psi_3 = \frac{x}{X}\frac{z}{Z} \qquad (14)$$

$$\psi_4 = \left(1-\frac{x}{X}\right)\frac{z}{Z} \qquad (15)$$

2.3 Evaluating the elemental matrix

The $\left[K^e\right]$ matrix

In other for us to solve for the K^e matrix which is the bearing matrix, we substitute the rectangular interpolation functions in eq. 12 to 15 accordingly into eq. 10. The results for the first to fourth elements, are shown in eq. 16-19 respectively.

$$\left[K^1\right] = \begin{pmatrix} \frac{7\cdot X}{48Z} - \frac{7\cdot Z}{48X} & \frac{X}{24Z} + \frac{7\cdot Z}{48X} & \frac{Z}{24X} - \frac{X}{24Z} & -\frac{7\cdot X}{48Z} - \frac{Z}{24X} \\ \frac{X}{24Z} + \frac{7\cdot Z}{48X} & \frac{X}{48Z} - \frac{7\cdot Z}{48X} & -\frac{X}{48Z} - \frac{Z}{24X} & \frac{Z}{24X} - \frac{X}{24Z} \\ \frac{Z}{24X} - \frac{X}{24Z} & -\frac{X}{48Z} - \frac{Z}{24X} & \frac{X}{48Z} - \frac{Z}{48X} & \frac{X}{24Z} + \frac{Z}{48X} \\ -\frac{7\cdot X}{48Z} - \frac{Z}{24X} & \frac{Z}{24X} - \frac{X}{24Z} & \frac{X}{24Z} + \frac{Z}{48X} & \frac{7\cdot X}{48Z} - \frac{Z}{48X} \end{pmatrix} \qquad (16)$$

$$\left[K^2\right] = \begin{pmatrix} \frac{X}{48Z} - \frac{7\cdot Z}{48X} & \frac{X}{24Z} + \frac{7\cdot Z}{48X} & \frac{Z}{24X} - \frac{X}{24Z} & -\frac{X}{48Z} - \frac{Z}{24X} \\ \frac{X}{24Z} + \frac{7\cdot Z}{48X} & \frac{7\cdot X}{48Z} - \frac{7\cdot Z}{48X} & -\frac{7\cdot X}{48Z} - \frac{Z}{24X} & \frac{Z}{24X} - \frac{X}{24Z} \\ \frac{Z}{24X} - \frac{X}{24Z} & -\frac{7\cdot X}{48Z} - \frac{Z}{24X} & \frac{7\cdot X}{48Z} - \frac{Z}{48X} & \frac{X}{24Z} + \frac{Z}{48X} \\ -\frac{X}{48Z} - \frac{Z}{24X} & \frac{Z}{24X} - \frac{X}{24Z} & \frac{X}{24Z} + \frac{Z}{48X} & \frac{X}{48Z} - \frac{Z}{48X} \end{pmatrix} \qquad (17)$$

$$[K^3]=\begin{pmatrix} \frac{7\cdot X}{48Z}-\frac{Z}{48X} & \frac{X}{24Z}+\frac{Z}{48X} & \frac{Z}{24X}-\frac{X}{24Z} & -\frac{7\cdot X}{48Z}-\frac{Z}{24X} \\ \frac{X}{24Z}+\frac{Z}{48X} & \frac{X}{48Z}-\frac{Z}{48X} & -\frac{X}{48Z}-\frac{Z}{24X} & \frac{Z}{24X}-\frac{X}{24Z} \\ \frac{Z}{24X}-\frac{X}{24Z} & -\frac{X}{48Z}-\frac{Z}{24X} & \frac{X}{48Z}-\frac{7\cdot Z}{48X} & \frac{X}{24Z}+\frac{7\cdot Z}{48X} \\ -\frac{7\cdot X}{48Z}-\frac{Z}{24X} & \frac{Z}{24X}-\frac{X}{24Z} & \frac{X}{24Z}+\frac{7\cdot Z}{48X} & \frac{7\cdot X}{48Z}-\frac{7\cdot Z}{48X} \end{pmatrix} \quad (18)$$

$$[K^4]=\begin{pmatrix} \frac{X}{48Z}-\frac{Z}{48X} & \frac{X}{24Z}+\frac{Z}{48X} & \frac{Z}{24X}-\frac{X}{24Z} & -\frac{X}{48Z}-\frac{Z}{24X} \\ \frac{X}{24Z}+\frac{Z}{48X} & \frac{7\cdot X}{48Z}-\frac{Z}{48X} & -\frac{7\cdot X}{48Z}-\frac{Z}{24X} & \frac{Z}{24X}-\frac{X}{24Z} \\ \frac{Z}{24X}-\frac{X}{24Z} & -\frac{7\cdot X}{48Z}-\frac{Z}{24X} & \frac{7\cdot X}{48Z}-\frac{7\cdot Z}{48X} & \frac{X}{24Z}+\frac{7\cdot Z}{48X} \\ -\frac{X}{48Z}-\frac{Z}{24X} & \frac{Z}{24X}-\frac{X}{24Z} & \frac{X}{24Z}+\frac{7\cdot Z}{48X} & \frac{X}{48Z}-\frac{7\cdot Z}{48X} \end{pmatrix} \quad (19)$$

The $\{F^e\}$ matrix

For the wedge F^e matrix, we substitute eq. 12 to 15 accordingly into eq. 11. The results for the first to fourth elements, are shown in eq. 20-23 respectively.

$$\{F^1\}=\begin{pmatrix} \frac{9\cdot X\cdot Z}{64} \\ \frac{3\cdot X\cdot Z}{64} \\ \frac{X\cdot Z}{64} \\ \frac{3\cdot X\cdot Z}{64} \end{pmatrix} \quad (20)$$

$$\{F^2\}=\begin{pmatrix} \frac{3\cdot X\cdot Z}{64} \\ \frac{9\cdot X\cdot Z}{64} \\ \frac{3\cdot X\cdot Z}{64} \\ \frac{X\cdot Z}{64} \end{pmatrix} \quad (21)$$

2.4 Assembly of the Element Equations

The assembly of finite element equations is based on two principles which can also be used for a one-dimensional problem. These are:

1. Continuity of primary variables
2. Equilibrium or balance of secondary variables.

Here, a quadrilateral element is used to analyse the domain. This quadrilateral is divided into four different rectangular elements as shown in the Figure 1. Let $K_{ij}^1(i,j=1,2,3,4)$ denote the coefficient matrix corresponding to the quadrilateral element.

$$\{F^3\}=\begin{pmatrix} \frac{3\cdot X\cdot Z}{64} \\ \frac{X\cdot Z}{64} \\ \frac{3\cdot X\cdot Z}{64} \\ \frac{9\cdot X\cdot Z}{64} \end{pmatrix} \quad (22)$$

$$\{F^4\}=\begin{pmatrix} \frac{X\cdot Z}{64} \\ \frac{3\cdot X\cdot Z}{64} \\ \frac{9\cdot X\cdot Z}{64} \\ \frac{3\cdot X\cdot Z}{64} \end{pmatrix} \quad (23)$$

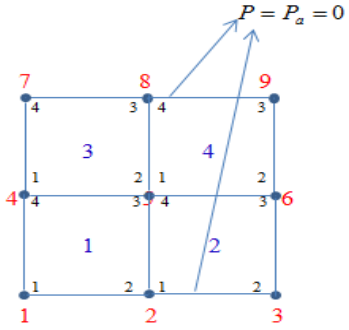

Figure 1. Four-element Mesh

The assembled K^e matrix is shown in eq. 24.

$$[K^e]=\begin{bmatrix} K_{11}^1 & K_{12}^1 & 0 & K_{14}^1 & K_{13}^1 & 0 & 0 & 0 & 0 \\ K_{21}^1 & K_{22}^1+K_{11}^2 & K_{12}^2 & K_{24}^1 & K_{23}^1+K_{14}^2 & K_{13}^2 & 0 & 0 & 0 \\ 0 & K_{21}^2 & K_{22}^2 & 0 & K_{24}^2 & K_{23}^2 & 0 & 0 & 0 \\ K_{41}^1 & K_{42}^2 & 0 & K_{44}^1+K_{11}^4 & K_{43}^1+K_{12}^4 & 0 & K_{14}^4 & K_{13}^4 & 0 \\ K_{31}^1 & K_{32}^1+K_{41}^1 & K_{42}^2 & K_{34}^1+K_{21}^4 & K_{33}^1+K_{44}^2+K_{11}^3+K_{22}^4 & K_{43}^2+K_{12}^3 & K_{24}^4 & K_{23}^4+K_{14}^3 & K_{13}^3 \\ 0 & K_{31}^2 & K_{32}^2 & 0 & K_{43}^1+K_{21}^3 & K_{33}^2+K_{22}^3 & 0 & K_{24}^3 & K_{23}^3 \\ 0 & 0 & 0 & K_{41}^4 & K_{42}^4 & 0 & K_{44}^4 & K_{43}^4 & 0 \\ 0 & 0 & 0 & K_{31}^4 & K_{32}^4+K_{41}^3 & K_{42}^3 & K_{34}^4 & K_{33}^4+K_{44}^3 & K_{43}^3 \\ 0 & 0 & 0 & 0 & K_{31}^3 & K_{32}^3 & 0 & K_{34}^3 & K_{33}^3 \end{bmatrix} \quad (24)$$

The assembled matrix is derived by substituting the results from the matrix in eq. 16 to 19 into eq. 24. The assembled bearing matrix is shown in eq. 25.

$$[K]=\begin{bmatrix}
\frac{7X}{48Z}-\frac{7Z}{48X} & \frac{2X}{48Z}+\frac{7Z}{48X} & 0 & -\frac{7X}{48Z}-\frac{2Z}{48X} & -\frac{2X}{48Z}+\frac{2Z}{48X} & 0 & 0 & 0 & 0 \\
\frac{2X}{48Z}+\frac{7Z}{48X} & \frac{2X}{48Z}-\frac{14Z}{48X} & \frac{2X}{48Z}+\frac{7Z}{48X} & 0 & -\frac{2X}{48Z}-\frac{4Z}{48X} & -\frac{2X}{48Z}+\frac{2Z}{48X} & 0 & 0 & 0 \\
0 & \frac{2X}{48Z}+\frac{7Z}{48X} & \frac{7X}{48Z}-\frac{7Z}{48X} & 0 & -\frac{2X}{48Z}+\frac{2Z}{48X} & -\frac{7X}{48Z}-\frac{2Z}{48X} & 0 & 0 & 0 \\
-\frac{7X}{48Z}-\frac{2Z}{48X} & -\frac{2X}{48Z}+\frac{2Z}{48X} & 0 & \frac{14X}{48Z}-\frac{2Z}{48X} & \frac{4X}{48Z}+\frac{2Z}{48X} & 0 & -\frac{7X}{48Z}-\frac{2Z}{48X} & -\frac{2X}{48Z}+\frac{2Z}{48X} & 0 \\
-\frac{2X}{48Z}+\frac{2Z}{48X} & -\frac{2X}{48Z}-\frac{4Z}{48X} & -\frac{2X}{48Z}+\frac{2Z}{48X} & \frac{4X}{48Z}+\frac{2Z}{48X} & \frac{4X}{48Z}-\frac{4Z}{48X} & \frac{4X}{48Z}+\frac{2Z}{48X} & -\frac{2X}{48Z}+\frac{2Z}{48X} & -\frac{2X}{48Z}-\frac{4Z}{48X} & -\frac{2X}{48Z}+\frac{2Z}{48X} \\
0 & -\frac{2X}{48Z}+\frac{2Z}{48X} & -\frac{7X}{48Z}-\frac{2Z}{48X} & 0 & \frac{4X}{48Z}+\frac{2Z}{48X} & \frac{14X}{48Z}-\frac{2Z}{48X} & 0 & -\frac{2X}{48Z}+\frac{2Z}{48X} & -\frac{7X}{48Z}-\frac{2Z}{48X} \\
0 & 0 & 0 & -\frac{7X}{48Z}-\frac{2Z}{48X} & -\frac{2X}{48Z}+\frac{2Z}{48X} & 0 & \frac{7X}{48Z}-\frac{7Z}{48X} & \frac{2X}{48Z}+\frac{7Z}{48X} & 0 \\
0 & 0 & 0 & -\frac{2X}{48Z}+\frac{2Z}{48X} & -\frac{2X}{48Z}-\frac{4Z}{48X} & -\frac{2X}{48Z}+\frac{2Z}{48X} & -\frac{2X}{48Z}+\frac{2Z}{48X} & \frac{2X}{48Z}-\frac{14Z}{48X} & \frac{2X}{48Z}+\frac{7Z}{48X} \\
0 & 0 & 0 & 0 & -\frac{2X}{48Z}+\frac{2Z}{48X} & -\frac{7X}{48Z}-\frac{2Z}{48X} & 0 & \frac{2X}{48Z}+\frac{7Z}{48X} & \frac{7X}{48Z}-\frac{7Z}{48X}
\end{bmatrix} \quad (25)$$

(25)

The assembled $\{F^e\}$ matrix is shown as follows,

$$\{F^e\}=\begin{Bmatrix} F_1^1 \\ F_2^1+F_1^2 \\ F_2^2 \\ F_4^1+F_1^4 \\ F_3^1+F_4^2+F_1^3+F_2^4 \\ F_3^2+F_2^3 \\ F_4^4 \\ F_3^4+F_4^3 \\ F_3^3 \end{Bmatrix} \quad (26)$$

$$\{F\}=\begin{Bmatrix} \frac{9XZ}{64} \\ \frac{6XZ}{64} \\ \frac{9XZ}{64} \\ \frac{6XZ}{64} \\ \frac{4XZ}{64} \\ \frac{6XZ}{64} \\ \frac{9XZ}{64} \\ \frac{6XZ}{64} \\ \frac{9XZ}{64} \end{Bmatrix} = \frac{XZ}{64}\begin{Bmatrix} 9 \\ 6 \\ 9 \\ 6 \\ 4 \\ 6 \\ 9 \\ 6 \\ 9 \end{Bmatrix} \quad (27)$$

Finally, substituting eqs. 25 and 27 into eq. 9, we have:
Substituting the values from eq. 20 to 23 accordingly into eq. 26, the resulting matrix is shown thus:

$$\begin{bmatrix}
\frac{7X}{48Z}-\frac{7Z}{48X} & \frac{2X}{48Z}+\frac{7Z}{48X} & 0 & -\frac{7X}{48Z}-\frac{2Z}{48X} & -\frac{2X}{48Z}+\frac{2Z}{48X} & 0 & 0 & 0 & 0 \\
\frac{2X}{48Z}+\frac{7Z}{48X} & \frac{2X}{48Z}-\frac{14Z}{48X} & \frac{2X}{48Z}+\frac{7Z}{48X} & 0 & -\frac{2X}{48Z}-\frac{4Z}{48X} & -\frac{2X}{48Z}+\frac{2Z}{48X} & 0 & 0 & 0 \\
0 & \frac{2X}{48Z}+\frac{7Z}{48X} & \frac{7X}{48Z}-\frac{7Z}{48X} & 0 & -\frac{2X}{48Z}+\frac{2Z}{48X} & -\frac{7X}{48Z}-\frac{2Z}{48X} & 0 & 0 & 0 \\
-\frac{7X}{48Z}-\frac{2Z}{48X} & -\frac{2X}{48Z}+\frac{2Z}{48X} & 0 & \frac{14X}{48Z}-\frac{2Z}{48X} & \frac{4X}{48Z}+\frac{2Z}{48X} & 0 & -\frac{7X}{48Z}-\frac{2Z}{48X} & -\frac{2X}{48Z}+\frac{2Z}{48X} & 0 \\
-\frac{2X}{48Z}+\frac{2Z}{48X} & -\frac{2X}{48Z}-\frac{4Z}{48X} & -\frac{2X}{48Z}+\frac{2Z}{48X} & \frac{4X}{48Z}+\frac{2Z}{48X} & \frac{4X}{48Z}-\frac{4Z}{48X} & \frac{4X}{48Z}+\frac{2Z}{48X} & -\frac{2X}{48Z}+\frac{2Z}{48X} & -\frac{2X}{48Z}-\frac{4Z}{48X} & -\frac{2X}{48Z}+\frac{2Z}{48X} \\
0 & -\frac{2X}{48Z}+\frac{2Z}{48X} & -\frac{7X}{48Z}-\frac{2Z}{48X} & 0 & \frac{4X}{48Z}+\frac{2Z}{48X} & \frac{14X}{48Z}-\frac{2Z}{48X} & 0 & -\frac{2X}{48Z}+\frac{2Z}{48X} & -\frac{7X}{48Z}-\frac{2Z}{48X} \\
0 & 0 & 0 & -\frac{7X}{48Z}-\frac{2Z}{48X} & -\frac{2X}{48Z}+\frac{2Z}{48X} & 0 & \frac{7X}{48Z}-\frac{7Z}{48X} & \frac{2X}{48Z}+\frac{7Z}{48X} & 0 \\
0 & 0 & 0 & -\frac{2X}{48Z}+\frac{2Z}{48X} & -\frac{2X}{48Z}-\frac{4Z}{48X} & -\frac{2X}{48Z}+\frac{2Z}{48X} & -\frac{2X}{48Z}+\frac{2Z}{48X} & \frac{2X}{48Z}-\frac{14Z}{48X} & \frac{2X}{48Z}+\frac{7Z}{48X} \\
0 & 0 & 0 & 0 & -\frac{2X}{48Z}+\frac{2Z}{48X} & -\frac{7X}{48Z}-\frac{2Z}{48X} & 0 & \frac{2X}{48Z}+\frac{7Z}{48X} & \frac{7X}{48Z}-\frac{7Z}{48X}
\end{bmatrix}
\begin{Bmatrix} P_1 \\ P_2 \\ P_3 \\ P_4 \\ P_5 \\ P_6 \\ P_7 \\ P_8 \\ P_9 \end{Bmatrix}
= -\frac{6\mu U}{h^3}\frac{\partial h}{\partial x}\frac{XZ}{64}
\begin{Bmatrix} 9 \\ 6 \\ 9 \\ 6 \\ 4 \\ 6 \\ 9 \\ 6 \\ 9 \end{Bmatrix} \quad (28)$$

But $X = \pi D, Z = \frac{L}{2}, U = \omega r$,

$h = c(1+\varepsilon\cos\theta)$ and $\frac{\partial h}{\partial x} = -c\varepsilon\sin\theta$ (29)

Substituting the parameters in eq. 28 and the boundary and initial conditions, we have:

$$\begin{bmatrix}
\frac{14X}{48Z}-\frac{2Z}{48X} & \frac{4X}{48Z}+\frac{2Z}{48X} & 0 \\
\frac{4X}{48Z}+\frac{2Z}{48X} & \frac{4X}{48Z}-\frac{4Z}{48X} & \frac{4X}{48Z}+\frac{2Z}{48X} \\
0 & \frac{4X}{48Z}+\frac{2Z}{48X} & \frac{14X}{48Z}-\frac{2Z}{48X}
\end{bmatrix}
\begin{Bmatrix} P_4 \\ P_5 \\ P_6 \end{Bmatrix}
= \frac{3\mu\omega L\pi r\varepsilon\sin\theta}{256c^2(1+\varepsilon\cos\theta)^3}
\begin{Bmatrix} 6 \\ 4 \\ 6 \end{Bmatrix} \quad (30)$$

3. Results and Discussion

The parameters used in this research are given below [21]:

μ=6.8Pa.s, ω=600rpm, c=0.000052*m*, ε=0.315, L=0.05*m*, D=0.1*m*

The results obtained as represented in the radar graph in Figure 2 shows the variation of pressure with angular displacements for a 2D journal bearing in which the effect of side leakage is considered. The nodal values are the pressures at those points on the The negative pressures in this regard are those that are below the ambient pressure. At this point, cavity begins to set in. This pressure increases in the negative direction till 225° and back again to the ambient pressure at 360°. Then, another cycle begins between 360 and 720 and so on.

bearing. The Newmann and the Dirichlet boundary conditions were used in the course of this research. The length to diameter ratio was 0.5. The result obtained from this research shows that the pressure increases from the ambient pressure which is taken to be zero at an angular displacement of 0° and increases significantly till 135°. At this point, the pressure becomes maximum. Thereafter, it begins to drop until it gets to180° where the pressure becomes the same as the ambient pressure. From this point onward, we begin to experience negative pressure.

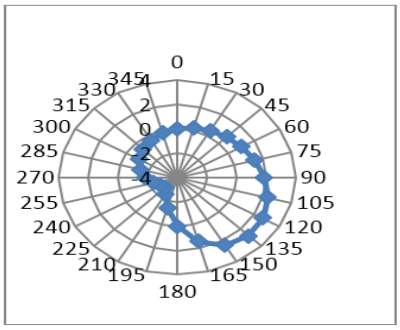

Figure 2. Graph of Pressure against angular displacement for 2D Journal Bearing

For an infinitely short journal bearing where the effect of side leakage was not considered, using the same parameters, the bearing pressure becomes maximum at145.3737^{o} and minimum at 210.6262^{o}. This difference in the position of the maximum and minimum pressure between the infinitely short journal bearing and the 2D journal bearing was as a result of the effect of the side leakage that was considered in the 2D journal bearing. For the maximum pressure, the experimental value obtained by [21] was 2.62Mpa and the predicted value from Raimondi and Boyd chart was 2.93Mpa. The inlet pressure, at the groove was maintained at 0.3MPa to ensure the continuity of oil supply. From this research, the maximum pressure obtained in the bearing was 2.80MPa. The result obtained shows a strong positive correlation between the experimental result and the result from the Raimondi and Boyd chart.

4. Conclusion

In this research, we have formulated the finite element based models for the classical Reynolds equation for the two dimensional Reynolds equation where the effect of end leakage is considered. The finite element method was used to successfully analyze the variation of pressure with the angular displacement of a lubricant in a journal bearing putting into consideration the effect of side leakage i.e., flow in the z-direction. The result obtained shows that the finite element method is an efficient and accurate method.

References

1. Budynas, RG.; Nisbett, JK. *Shigley's Mechanical Engineering Design*, 8th Edition. McGraw-Hill: **2008**.
2. Nuruzzaman, DM.; Khalil, MK.; Chowdhury, MA.; Rahaman, ML. Study on pressure distribution and load capacity of a journal bearing using finite element method and analytical method. *International Journal of Mechanical & Mechatronics Engineering IJMME-IJENS*, **2010**, *10*(5), 1-8.
3. Gustavo, GV. Daniel, OB.; Lidia, MQ. Approximate analytical approximate solution to Reynolds equation for finite length journal bearings. *Tribology International*, **2011**, *44(10)*, 1089-1099.
4. Benasciutti. D.; Gallina, M.; Munteanu, G.; Flumian, F. A numerical approach for the analysis of deformable journal bearings, *Frattura ed Integrità Strutturale*, **2012**, *21*, 37-45.
5. Dwivedi, VK.; Sanjeev KG.; Deepti, S.; Pratibha, S.; Bhupendra S. Effect of eccentricity ratio on pressure profile of short journal bearing. *Proceeding of 1st International Conference on Innovative Technologies in Mechanical Engineering*, **2012**, 225-230.
6. Dwivedi, VK.; Gupta KS. Finite difference method analysis of hybrid bearing. *5th International Conference on Advances in Mechanical Engineering*, **2011**, 240 - 244.
7. Navthar, RR.; Halegowda, NV.; Deshpande, S. Pressure distribution analysis of hydrodynamic journal bearing using artificial neural network. *International Conference on computer & automation Eng. 4th (ICCAE2012)*, **2012**.
8. Sfyris, D.; Chasalevris, A. An exact analytical solution of the Reynolds equation for the finite journal bearing lubrication. *Tribology International*, **2012**, *55*, 46-58.
9. Mane, RM.; Soni, S. Analysis of hydrodynamic plain journal bearing. *Excerpt from the proceedings of the COSMOL Conference*. Bangalore: **2013**. https://www.comsol.com/paper/download/182933/mane_paper.pdf
10. Marco, TCF. On the hydrodynamic long journal bearing theory. *Proceedings of the World Congress on Engineering*, **2014**, *(2)*.
11. Priyanka, T.; Veerendra, K. Analysis of hydrodynamic journal bearing using CFD and FSI technique. *International Journal of Engineering Research & Technology*, **2014**, *3*, 1210-1215.

12. Paras, K; Ashish, KG. Experimental investigation on hydrodynamic journal bearing using SAE 10W30 multi grade oil. *International Journal of Advance Research and Innovation*, **2014**, *2(1)*, 166-173.
13. Gustafson T.; Rajagopal, KR.; Stenberg, R.; Videman, J. Nonlinear Reynolds equation for hydro dynamic lubrication. *Applied Mathematical Modelling*, **2015,** *39*, 5299–5309.
14. Francisco, JP.; Matteo, G.; Demetrio, CZ.; Daniele, D. A general finite volume method for the solution of the Reynolds lubrication equation with a mass-conserving cavitation model. *Tribology Letter*, **2015**, *60*(18), 1-21.
15. Fu, Y.; Zhou, X.; Guo, H.; Mei, P. Lubrication analysis of journal bearings in R410A rotary compressor. *23rd International Compressor Engineering Conference at Purdue*, July 11-14, **2016**, Paper 2509.
16. Verma, A.; Samant, SS. Inspection of hydrodynamic lubrication in infinitely long journal bearing with oscillating journal velocity. *Journal of Applied Mechanical Engineering*, **2016**, *5(3)*, 1-7.
17. Muzakkir, SM. Methodology for the control of wear of journal bearing operating in mixed lubrication regime. *International Journal of Applied Engineering Research*, **2016**, *11*, 665-668.
18. Shinde, PD.; Nagare, PN. Experimental evaluation of performance parameters of journal bearing operating in boundary/ mixed lubrication regimes. *International Advance Research Journal of Science*,**2016**, *3*(SI 1), 116-120.
19. Manojkumar; Shamburaje; Rameshwar. CFD analysis of elasto hydro-dynamic lubrication journal bearing using castor oil and bronze material. *International Journal of Advance Research and Innovative Ideas in Engineering*, **2016**, *2*(2), 56-67.
20. Hamdavi, S.; Ya, HH.; Rao, TVVLN.; Faez, KM. An analytical approach to investigate the effect of grooved surface on short journal bearing's performance. *ARPN Journal of Engineering and Applied Science*, **2016**, *11(20)*, 12045-12049.
21. Ahmad, MA.; Salmiah, K;, Rob-Dwyer J.; Che, FMT. Preliminary study of pressure profile in hydrodynamic lubrication journal bearing. *International Symposium on Robotics and Intelligent Sensors*, **2012**, *41*, 1743-1749.